BNL-229645-2026-TECH

C-A/AP-1111

Study of a Fixed Field Accelerator as a Driver for Proton Driven Plasma Wakefield Acceleration

F. Willeke

April 2026

Collider Accelerator Department

Brookhaven National Laboratory

U.S. Department of Energy

USDOE Office of Science (SC), Nuclear Physics (NP)

DISCLAIMER

Study of a Fixed Field Accelerator as a Driver for Proton Driven Plasma Wakefield Acceleration

F. Willeke, Brookhaven National Laboratory, Brookhaven, US

Abstract:
A fixed field accelerator (FFA) scheme is studied that is aimed to provide a continuous stream of high-energy proton bunches at a rate of up to $20\,kHz$. The bunches can be used to drive plasma wakefields capable of acceleration of leptons in a single stage for a lepton collider at the Higgs and the top-mass scales. The proposed FFA is assumed to have a circumference of $6900\,m$ and is designed to accelerate proton bunches from $150\,GeV$ to $500\,GeV$.

I. INTRODUCTION

Experiments at CERN have successfully demonstrated the acceleration of electrons in plasma wakefields driven by $400\,GeV$ proton bunches from the Super Proton Synchrotron (SPS) [1]. Encouraged by these results, concepts are currently being developed to exploit this technique for a high–center-of-mass-energy lepton collider operating in the Higgs- and top-quark energy scales. The ALIVE collaboration [2] has been initiated to develop such concepts.

Plasma wakefields can sustain acceleration gradients of more that one order of magnitude higher than those achievable with conventional radio-frequency (RF) acceleration. A key advantage of proton driven plasma wakefield acceleration using proton energies of several hundred GeV, over laser- or electron-beam-driven schemes is the enormous energy stored in a single proton bunch. This substantial energy reservoir may not be fully depleted even when electrons are accelerated to energies of $150\,GeV$ or beyond. Consequently, lepton acceleration can in principle be achieved in a single stage, eliminating the need for repeated disposal of a depleted drive beam and injection of a fresh one. Such staging represents a major technical challenge for laser- or electron-driven plasma wakefield accelerators operating at very high energies [3].

Another advantage of the proton driven plasma wakefield accelerator is the potential use of existing infrastructure such as accelerator tunnels, particle sources, power distribution and cooling systems. Compared to storage rings and linear colliders, the facility has a moderate overall footprint.

In addition to center-of-mass energy, luminosity is a critical collider performance parameter. The luminosity of an $e^+ - e^-$ collider is proportional to the collision rate of electron–positron bunch pairs. To achieve a competitive collider design based on proton driven plasma wakefield acceleration, the proton drive bunches must therefore be delivered at a high repetition rate.

Synchrotrons are the most efficient machines for accelerating protons to high energies, since they can accelerate many bunches simultaneously, enabling a high intensity, high-energy proton beam. However, their cycle rate is limited not only by the magnet ramp rate constraint, for example by eddy currents, high inter-coil and coil-to-ground voltage, power supply requirements, and circuit tracking - but also by the time required to inject many bunches into the machine by using a chain of smaller, lower-energy synchrotrons with a limited repetition rate. These constraints reduce the achievable luminosity compared with collider concepts, such as storage rings or linear colliders.

The limited proton drive bunch production rate motivates the exploration of fixed field accelerators (FFAs) for proton acceleration.

Accelerators with fixed magnetic fields, such as cyclotrons and microtrons, are among the earliest particle accelerator concepts. They are most attractive in the energy range of below a few GeV. Fixed field alternating-gradient accelerators (FFAGs), proposed in the 1950s [5], employ magnetic fields with strong radial dependence and can, in principle, accommodate somewhat larger energy ranges. Nevertheless, FFAGs have historically been unable to compete with synchrotron technology due to their more complex and less efficient magnet systems and their limited energy reach. For multi-GeV energy gains which require many turns or repeated passage through RF accelerating cavities, the FFA magnetic lattice becomes increasingly inefficient, as discussed below. Consequently, fixed field accelerators have historically been confined to low- and medium-energy applications.

Despite these limitations, the specific requirements of a proton driver for plasma wakefield generation may justify accepting the inefficiencies of a fixed field magnet system in exchange for substantially larger high-energy proton bunch rates. Such high proton bunch rates could enable the high collision frequencies of high energy leptons required for a competitive high-energy lepton collider.

There is another aspect which adds to the advantage of an FFA: As is discussed below, acceleration in an

FFA allows to extract very short proton bunches from the accelerator which is essential to obtain the desired large plasma wakefields for electron acceleration.

In the following sections, we will explore how an FFA could operate in this very high energy regime. Section II develops the basic considerations for proton drive beam generation. Section III states the requirements and design goals. Section IV describes a model lattice for proton energies between $150\,GeV$ and $500\,GeV$. Section V presents an optimization of acceleration and bunch compression parameters. Section VI, assesses the dynamic aperture, a critical aspect of high-energy FFA performance. Section VII, discusses the superconducting magnet design. Section VIII provides a brief assessment of the RF system, and Section IX describes the injection and extraction schemes. Section X outlines the proposed path forward, followed by the conclusions.

II. BASIC CONSIDERATIONS ON FIXED FIELD ACCELERATORS FOR PROTON DRIVE BEAM GENERATION

An FFA can, in principle, produce a continuous stream of equally spaced proton bunches. The high-energy FFA considered here employs an alternating-gradient combined-function magnet lattice. The magnetic field varies with radial position within the aperture, ranging from the value required at injection to the value corresponding to the maximum beam energy. The beam energy is provided by RF cavities, and the RF phase ϕ is maintained close to 0° in order to maximize the per-turn energy gain,

$$\Delta E_n/\text{turn} = U_{RF}\cos(\phi_n),$$

where n labels the turns around the accelerator.

Two types of FFAs are commonly distinguished.

Non-scaling FFAs feature a varying ratio between the bending and focusing fields from turn to turn. As a result, the betatron tunes change continuously during acceleration. Operation near integer betatron resonances must be avoided to maintain beam stability. This concept is suitable for very rapid acceleration over a limited number of turns, effectively "jumping" across integer resonances. However, for proton acceleration by several hundred GeV, the required RF voltage would be prohibitively large.

For an FFA to be viable as a driver for high-energy protons generating plasma wakefields for the acceleration of electrons to $150\,GeV$, the total circumferential RF voltage must be much smaller than $150\,GV$. In practice, the circumferential RF voltage should not exceed a few hundred MV. This constraint implies approximately 10^3 turns of acceleration in the FFA. Under such conditions, the gradual variation of the betatron tune would lead to repeated proximity to integer resonances, with potentially catastrophic consequences for beam stability.

For this reason, we consider the second type, the scaling FFA. In a rectangular curved magnet implementation, scaling requires the ratio of the integrated focusing and bending fields to remain constant across the radial coordinate x. (Note that rectangular curved magnets are typical for high energy accelerators whereas in low energy machines a more common choice is sector non-curved magnets which has implication for how the magnetic field changes radially and along the beam trajectory).

$$\frac{1}{B_y}\frac{dB_y}{dx} = \text{constant}. \tag{1}$$

This condition implies an exponential variation of the bending field across the radial coordinate in the magnet aperture,

$$B_y(x) = B_y(x_{inj})\exp\left(\frac{x - x_{inj}}{\Delta x}\right), \tag{2}$$

where x_{inj} is the radial position at injection, which can be taken as zero.

The focusing gradient G_y is determined by the parameter Δx and is given by

$$\frac{dB_y(x)}{dx} = G_y(x) = \frac{B_y(x_{inj})}{\Delta x}\exp\left(\frac{x}{\Delta x}\right). \tag{3}$$

The bending radius ρ of the magnets remains constant during acceleration,

$$\frac{1}{\rho} = \frac{ecB_y(x)}{E\beta} = \frac{eeB_y(x_{inj})}{E_{inj}\beta_{inj}}, \tag{4}$$

where $\beta = v/c$.

The focusing strength

$$k_{foc} = \frac{ecG_y(x)}{E\beta} = \frac{G_y(x)}{B_y\rho} = \frac{1}{\Delta x_f \rho} \tag{5}$$

also remains constant during acceleration.

Stable beam optics requires alternating field gradients. Since the gradients and bending fields are proportional, the bending fields must alternate as well. Thus, their sign alternates between horizontally focusing and vertically focusing (horizontally de-focusing) magnets, such that $\rho_d = -\rho_f$. Equal focusing in the horizontal and vertical plane would therefore produce an undulating orbit along a straight trajectory. Net inward bending is obtained by making the horizontally focusing magnets stronger than the vertically focusing ones, so that the net bending exceeds the anti-bending contribution.

However, the permissible ratio between vertical and horizontal focusing is limited by optical stability. Denoting the ratio of vertical to horizontal focusing by κ, and assuming similar bending radii and focusing strengths

but different magnetic lengths $L_d = \kappa L_f$, the relationship between the peak and average bending fields becomes

$$B_{peak} = \frac{1+\kappa}{1-\kappa} B_{av}. \quad (6)$$

Here

$$B_{av}(E) = \frac{2\pi E}{ecC\eta},$$

where η is the magnetic fill factor and C is the circumference of the accelerator ring (at injection energy).

This relation implies that the peak magnetic fields are significantly larger than the average bending field that would be required in a synchrotron of the same energy and circumference. Consequently, the achievable beam energy is strongly constrained by the maximum attainable magnetic field.

III. REQUIREMENTS

In order to generate the envisioned plasma wakefields for accelerating electrons to $150\,GeV$ and beyond, short and intense high energy proton bunches are required. We base this study on a peak proton energy of $500\,GeV$, a proton intensity of 10^{11} (16 nC) protons per bunch, and aim for a RMS bunch length of $1\,mm$. We assume a longitudinal emittance of $\varepsilon = 0.3\,eV sec$ at injection with an initial RMS bunch length of $5\,cm$. For an $e^+ - e^-$ collider with competitive luminosity, we require a proton bunch repetition frequency of at least $10\,kHz$.

IV. ACCELERATOR LATTICE AND BEAM OPTICS

The solution considered here is based on a circumference of $6900\,m$. (Accelerator tunnels of this size exist with some of them serving no purpose at this time). The accelerator lattice is composed of curved rectangular combined function magnets with alternating gradients. The beam trajectory in these magnets are segments of a circular orbit that are identical at all beam energies. The angles of input and output trajectories with respect to the faces of the magnet are both half the bend angle $\theta_{f,d} = L_{f,d}/|\rho|$ but are different for focusing and defocusing magnets.

The ratio of the length of vertically focusing and horizontally focusing magnets is $\kappa = 0.65$. This value provides a stable and robust beam optics. It is close to the minimum value compatible with a periodic optical solution. We use horizontally focusing magnets of length $L_f = 2.360\,m$ that are bending inwards, and vertically focusing magnets of length $L_d = 1.5345\,m = 0.65 \cdot L_f$ that are bending outwards. They are separated by a drift space of $L_{dr} = 0.4852\,m$ at injection energy. The magnetic fill factor is assumed to be $\eta = 0.7$. The straight sections for RF, injection and extraction elements totaling $L_{str} = 867\,m$. The bending radius averaged over horizontally and vertically focusing magnets is $\rho_{av} = \eta \cdot C/(2\pi 0 = 768.71\,m$. The bending radius in both horizontally and vertically focusing magnets is $\rho = \pm\eta C/(2\pi) \cdot (1-\kappa)/(1+\kappa) = \pm 163.06\,m$ and the bending angles are $\theta_f = L_f/\rho = 14.48\,mrad$ and $\theta_d = -L_d/\rho = -9.41\,mrad$ and are constant for all energies. The bending field varies exponentially with radial excursion x and so does the corresponding beam energy. The choice of Δx_f is $12.4\,mm$. It is slightly smaller in the de-focusing magnets. It determines the strength of the focusing $k_{foc} = 1/(\Delta x_f \rho) = 0.5068 m^{-2}$. The beam will move during acceleration radially in the aperture of the horizontally focusing magnets with a maximum excursion of

$$x_f = \Delta x_f \cdot ln\,(B_{fin}/B_{inj}) = 14.5683\,mm, \quad (7)$$

where $B_{inj} = E_{inj}\beta/(ec\rho)$ and $B_{fin} = E_{inj}\beta/(ec\rho)$ are the magnetic field values at injection and final energy. The corresponding radial position change in the de-focusing magnet, x_q is slightly smaller

$$x_d = x_f \cdot cos(\theta_f/2)/cos(\theta_d/2) = 14.5680\,mm \quad (8)$$

Intermediate values of x are given by

$$x(E) = \Delta x_f \cdot ln\,(B/B_{inj}) = \Delta x_f \cdot ln\,(E/E_{inj})\,. \quad (9)$$

The magnetic field varies between

$$B_y(E_{inj}) = \frac{E_{inj} \cdot \beta_{inj} \cdot \eta \cdot C}{2\pi \cdot e \cdot c} \cdot \frac{1+\kappa}{1-\kappa} = 3.068T \quad (10)$$

and

$$B_y(E_{fin}) = \frac{E_{fin} \cdot \beta_{fin} \cdot \eta \cdot C}{2\pi \cdot e \cdot c} \cdot \frac{1+\kappa}{1-\kappa} = 10.228T \quad (11)$$

The drift space between magnets changes slightly with radial excursion Δx_f for focusing and de-focusing magnets with a maximum value:

$$\Delta s = x_f \cdot sin\left(\frac{\theta_f}{2}\right) - x_d \cdot sin\left(\frac{\theta_d}{2}\right) \quad (12)$$

The change in drift lengths with radial offset Δx_f for each cell amounts to $\Delta s = 0.0557\,mm$. Figure 1 depicts schematically the periodic cell structure.

It should be pointed out that the tune is not exactly constant during acceleration, as the path length through the magnet system changes slightly for different radial positions of the beam. But for the large energy application with small deflection angle per magnet that we are considering, this effect is negligibly small, in fact much smaller than the effect of unavoidable magnetic imperfections.

The beam optical parameters of this FODO cell structure is as follows:

- maximum and minimum $\beta_x : 11.836\,m, 0.403\,m$

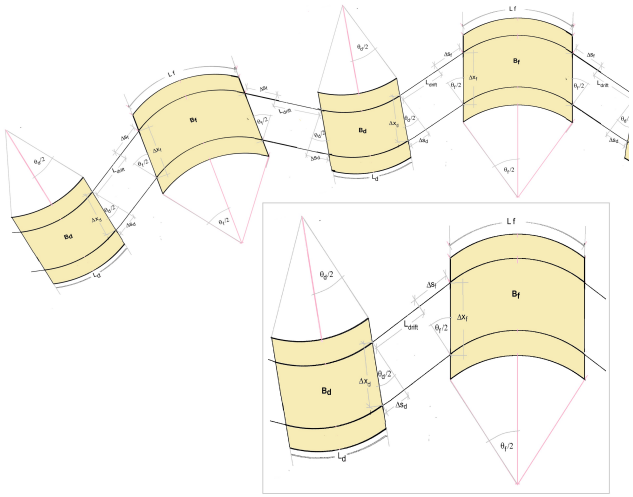

FIG. 1. Schematic geometry of the FFA. Note that the bend angles and drift spaces are strongly exaggerated.

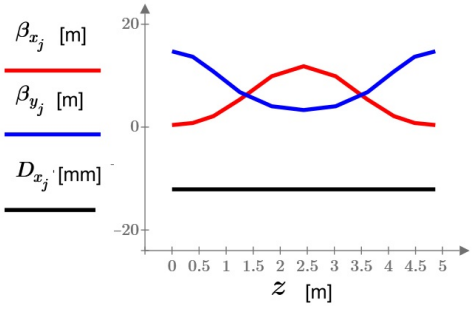

FIG. 2. Beam Optics function of a periodic cell

- minimum and maximum β_y : $4.055\,m, 14.437\,m$
- initial and final ΔQ_x : 0.42115, 0.42117
- initial and final ΔQ_y : 0.12631, 0.12633
- $\gamma_T = 282.67$

Figure 2 shows the lattice function of a periodic cell. The value of the dispersion is small because of the difference in vertical and horizontal bending and focusing and the difference in length of horizontally and vertically focusing magnets.

The accelerator lattice needs to include straight sections for RF cavities, injection and extraction elements and other utilities. It would exceed the scope of this study to work out a detailed accelerator lattice. However, the following concept of how to design such a lattice is helpful for future efforts. The challenge of designing a lattice for this FFA is that the structure of bends and focusing is strongly correlated. This is made particular challenging since the desire to preserve one of the strong advantages of the proton driven plasma

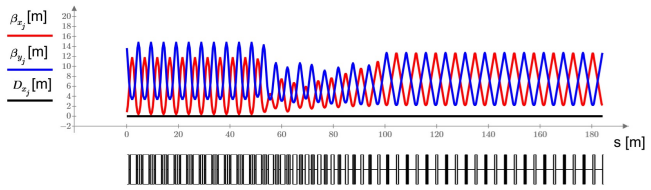

FIG. 3. Transition of lattice structure and beam optics from the periodic arc structure to the periodic straight section structure

wakefield acceleration based collider namely the use of existing infrastructure, in particular the use of an existing accelerator tunnel. Thus, varying the quadrupoles in order to transition from the periodic arcs into the straight section implies a sequence of bending fields that may render the beam orbit outside the accelerator tunnel. The following concept is envisioned to overcome such difficulty: The straight sections are constituted by bending and anti-bending magnets of equal strength and focusing and anti-focusing. This implies equal focusing in the horizontal and vertical plane. Furthermore, there need to be drift spaces between these magnets for the equipment to be accommodated.

The following concept is applied for the transition from arcs to straight sections: From FODO cell to FODO cell, the lengths of magnets and straight section is modified in small steps to transition from the arc to the straight section structure. There are further requirements: The straight and transition sections should not negatively impact the transverse dynamic and the dynamic aperture. There is a limited number of free parameters to accomplish this which defines an interesting optimization problem. Figure 3 depicts the transition from the periodic arc cell structure to the periodic straight section cell structure. Starting from the periodic beam optics in the arcs, the lengths of the straight section in the transition region is fine-tuned to match the beam optics to the periodic solution of the straight section. The magnet strength remains the same. The final length of magnets in the arcs is $80\,cm$. The straight sections in between are $3\,m$ long.

Note that the dispersion is small ($D_x \simeq 12\,cm$) and is almost constant. The slope of the dispersion is very close to zero in the middle of the straight section such that the arc value remains periodic in a complete ring design in the same fashion.

The design so far does not pretend to constitute a complete design of the FFA lattice. This requires to take into account the existing tunnel geometry which at this point is not yet determined.

V. ACCELERATION AND BUNCH COMPRESSION

The study presented here is based on an FFA for acceleration of protons between $E_{inj} = 150\,GeV$ and $E_{fin} = 500\,GeV$ in a $C = 6900\,m$ long circular accelerator tunnel. The acceleration time corresponds to $N_{turn} \simeq 700$ turns around the accelerator. This requires a large RF circumferential voltage of

$$U_{rf} \simeq \frac{E_{final} - E_{ini}}{e \cdot N_{turn}} \simeq 700\,MV \tag{13}$$

The revolution time changes during acceleration. There are two effects: As the beam moves outwards during acceleration, its path length changes in each FODO cell according to equation 12 with radial excursions x_f and x_d given by equations 7,8:

$$\Delta s(E) = ln\left(\frac{E}{E_{inj}}\right)\left(\Delta x_f sin\left(\frac{\theta_f}{2}\right) - \Delta x_d sin\left(\frac{\theta_d}{2}\right)\right) \tag{14}$$

Furthermore, the beam velocity changes according to

$$v_p(E) = c \cdot \sqrt{1 - \left(\frac{E_{rp}}{E}\right)^2} \tag{15}$$

($E_{rp} = 938.2721\,MeV$ is the rest energy of the proton) This changes the revolution time by

$$T_{rev}(E) = (C + \Delta s(E) \cdot N_{cell}) \cdot v_p(E)^{-1}, \tag{16}$$

where $N_{cell} = 2\pi/(\theta_f - \theta_d)$ is the number of arc-FODO cells. Figure 4 shows the evolution of the revolution time. The revolution time is given by the beam energy and the design of the FODO cell structure. It is only approximately constant as a function of energy. Thus, the RF phase will change during acceleration and so do acceleration rate and accelerating gradient (longitudinal focusing). The choice of a low RF frequency that must remain constant, will mitigate the variation of RF frequency. However, with lower RF frequency it will be more difficult to obtain the large accelerating voltage of the FFA. The choice of $f_{RF} = 52\,MHz$ appears to be a possible compromise between these conflicting requirements. The harmonic number is $h = 1200$.

In order to minimize the impact of the revolution time change on the RF phase and to set up the accelerator for a smooth efficient acceleration, the RF-frequency is fine-tuned and the initial RF phase is optimized to mitigating the impact of the residual change in revolution time (see Figure 4) and corresponding RF phase shift during the acceleration process. The RF frequency that matches the revolution time at injection energy $T_{rev}(E_{inj}$ is $f_{RF}^{opt} = h/(C \cdot T_{rev}(E_{inj}) = 52.134377\,MHz$. The optimum RF frequency is $f_{RF} + 0.6316\,kHz$). The optimum initial RF phase is $\phi_0 = 0.26 \cdot \pi$.

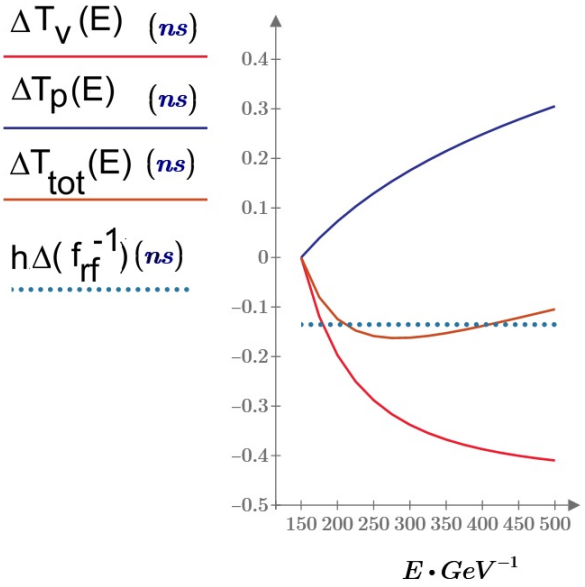

FIG. 4. Evolution of the revolution time with beam energy: The upper graph (in blue) shows the path length effect by keeping the velocity artificially at the injection level. In the lower graph (in red), the path length is kept artificially at the injection level. The third graph (in green) shows the combined effect. The dotted line indicates the choice of the RF frequency that is the same for all energies.

The evolution of beam energy as a function of turns in the accelerator, E_n is given by the following recursion formula

$$E_n = E_{n-1} + e \cdot U_{rf} \cdot cos(2\pi \cdot f_{rf} \cdot \sum_{m=0}^{n-1} T_{rev}(E_m)) \tag{17}$$

The evolution of the beam energy E_n of a single particle launched at the injection energy is shown in Figure 5 and the corresponding evolution of the RF phase is depicted in 6. The beam energy reaches a top of $567\,GeV$ after 900 turns before the particle is decelerated. The RF phase remains between $-90°$ and $90°$. $500\,GeV$ is reached after 760 turns.

The acceleration of a proton beam has been simulated using 10^3 randomly distributed test particles. It is assumed that each test particle is launched on an orbit denoted by $x(E)$ (see equation 9) corresponding to its individual injection energy E. This can be accomplished be the correct amount of dispersion of the injection line at the launch point. The bunch is assumed to have a relative RMS energy spread of $\Delta E/E = 10^{-3}$ and a RMS bunch length of $50\,mm$. The corresponding longitudinal invariant emittance is $A = 0.0301\,eV sec$. These parameters correspond to bright beam parameters that can be achieved today. The individual particles in the bunch have different revolution times according to their individual energy and the bunch length consequently increases

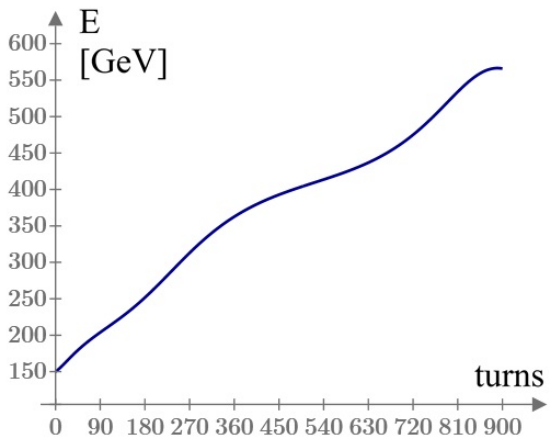

FIG. 5. Energy of the reference particle as a function of turns in the accelerator ring

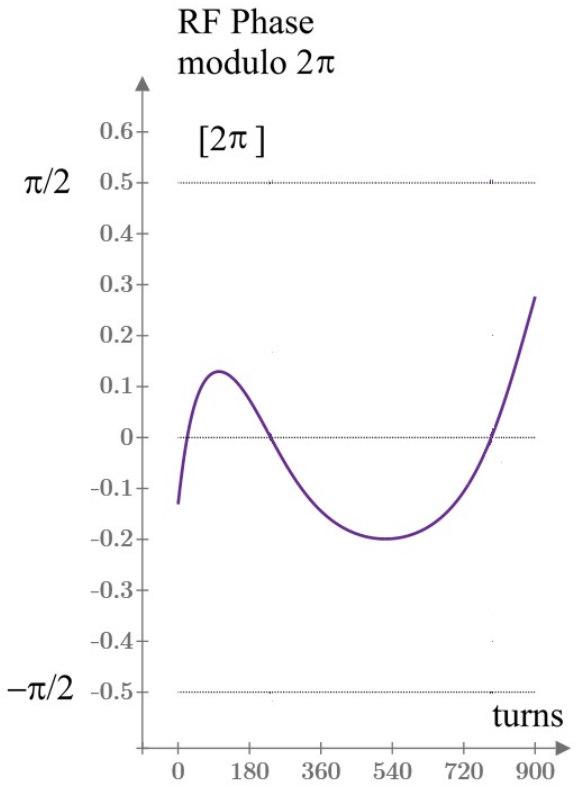

FIG. 6. Evolution of the RF phase during acceleration

strongly during acceleration. At the same time, the head and the tail of the bunch experience different energy gain. However, the emittance of the bunch is preserved. Figure 7 depicts the phase space before and after acceleration. The synchrotron frequency of the FFA varies between 55

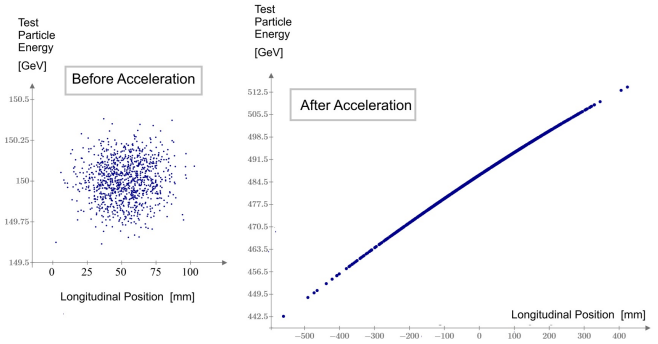

FIG. 7. Longitudinal phase space of the bunch of test particles before acceleration (150 GeV) and after acceleration (450 GeV).

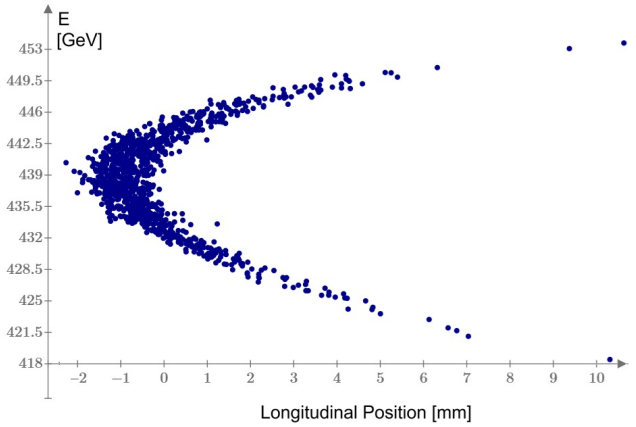

FIG. 8. Longitudinal phase space of the bunch of test particles after compression

Hz at injector to 30 Hz at top energy. The total acceleration time is only 8 ms. Thus the particles perform only 0.75 synchrotron oscillations during the ramp. In order to obtain required the short bunch length required for strong plasma wakefield generation, the bunch is extracted at the 600^{th} turn. It has an average energy of $E_{extr} = 427GeV$. The bunch is then injected into a compressor ring which is assumed to have a similar circumference $C = 6900\ m$ and which is assumed to have a momentum compaction factor of $\alpha_{comp} = -0.00767$. The phase space of the bunch compressed that way in one turn is shown in Figure 8. The RMS bunch length after completion of one turn in the compressor ring amounts to $\sigma_s = 1.16\,mm$ (this value is obtained by cutting the distribution at 97.4% of the particles). The distribution is shown in Figure 9.

VI. DYNAMIC APERTURE

The exponential rise of the magnetic bend field in the aperture corresponds to a considerable nonlinear field dis-

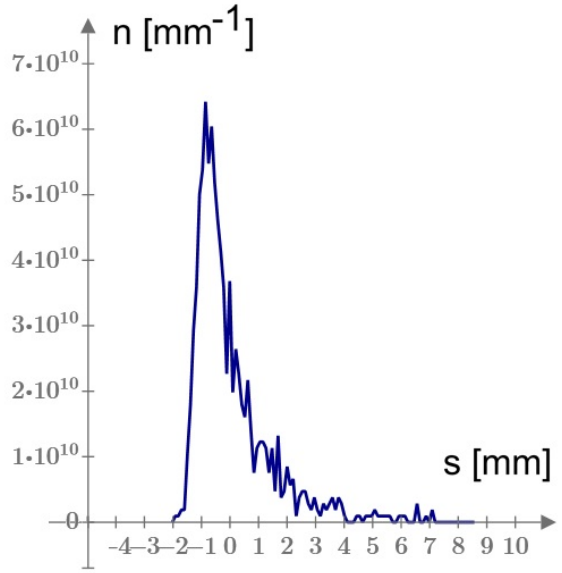

FIG. 9. Particle distribution after compression. The RMS bunch length is $\sigma_b \simeq 0.9\,mm$. The density function was extrapolated from 10^3 test particles to the full bunch population of 10^{11} protons.

tortion of the linear beam optics that considers only the dipole and quadrupole component. This concern is addressed by a tracking calculation. The two-dimensional nonlinear field is described by a multipole expansion up to do-decapole terms. It is taken into account in the tracking calculation by inserting a thin-lens nonlinear element in the middle of each dipole. The thin lens element inside the focusing (f) and de-focusing (d) magnets is described by the following expression:

$$\Delta_x(x,y) = \theta_{f,d} \sum_{n=2}^{6} \sum_{k\,even}^{n} \frac{1}{(n-l)!k!}(-1)^{k/2}\frac{x^{n-k}y^k}{\Delta x_f^n}$$
$$\Delta_y(x,y) = \theta_{f,d} \sum_{n=2}^{6} \sum_{k\,odd}^{n} \frac{1}{(n-l)!k!}(-1)^{(k-1)/2}\frac{x^{n-k}y^k}{\Delta x_d^n} \quad (18)$$

where Δ_x is the kick applied in the x-direction and Δ_y is the kick applied in the y-direction. In a first step of exploring transverse dynamics, the beam energy change is accounted for by multiplying the particle trajectory slopes by the adiabatic damping factor E_{n-1}/E_n. The energies E_n are obtained from independent longitudinal tracking. We track a single particle with an equivalent amplitude in x and y. We assume an equal transverse beam emittance of $\epsilon_t = 6.7\,nm$ in both planes. The maximum initial amplitudes which allow particles to be

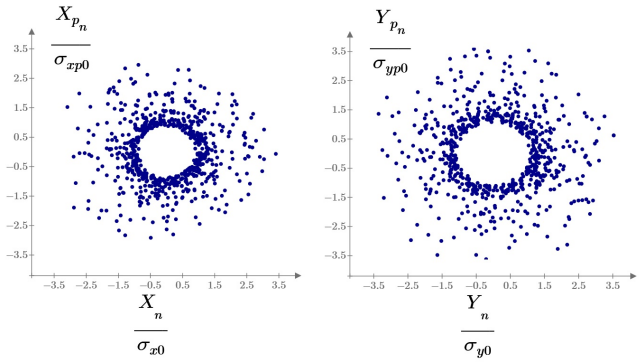

FIG. 10. Result of single particle transverse tracking taking into account the non-linearity of the exponential field characteristics.

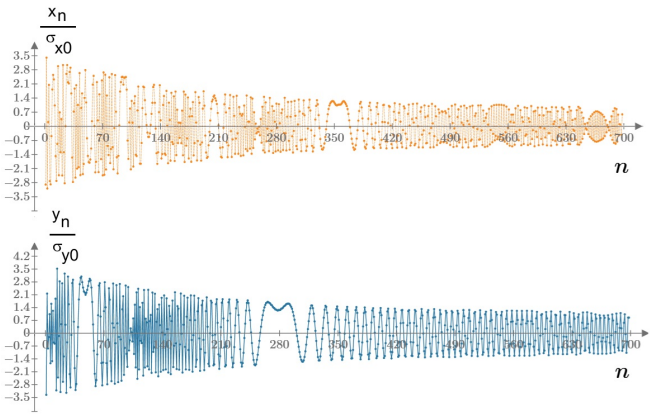

FIG. 11. Turn-by-Turn diagram of tracking results

accelerated to the top energy are found as

$$x_0 = 3.6 \cdot \sqrt{\epsilon_t \cdot \beta_{x0}}$$
$$y_0 = 3.6 \cdot \sqrt{\epsilon_t \cdot \beta_{y0}}. \quad (19)$$

Results of the tracking are shown in Figure 10. Figure 11 show the particle betatron amplitudes versus number of revolution. The dynamic aperture is found to be 5.1 rms beam sizes. This is not generous as no errors are taken into account. There is the possibility to introduce nonlinear correction fields.

VII. FIXED FIELD ACCELERATOR MAGNET

The Fixed Field Accelerator magnets are challenging components beyond the state of the art.

The requirements are demanding: The ratio of quadrupole and dipole fields need to be constant to a fraction of 1% over the entire aperture to avoid that the accelerator tune changes during acceleration. As there are $N_{cell} \simeq 1500$ cells, the cell tune needs to be held constant to $\Delta Q_{cell} \simeq 1/N_{cell} < (6-7)\cdot 10^{-4}$ to keep the

tune change within an integer during acceleration.

Furthermore, the magnets should not only be feasible but also manufacturable in a mass-producing fashion.

In order to explore these challenges, a model magnet is developed.

The model magnet is based on the superposition of multipole coils. A total number of six multipoles, from dipole to do-decapole provides sufficiently constant quadrupole strength $\Delta k = \frac{G_y}{\rho B y} < 10^{-4}$ over the 16 mm aperture.

The model magnet is based on a technique called direct-wind [4]. Superconducting wires are positioned on an epoxy-coated cylinder and fixed in place by applying ultrasonic power. This technique can be automatized, which is a major advantage of this technology. For a multilayer coil each layer can correct errors that occur in the previous layer. This way excellent field quality can be achieved, in principle. It should be pointed out that the present state of the technology allows only magnetic fields in the order of $3-4\,T$. Furthermore, the conductors that can provide the current density required for such a magnet also need substantial R&D.

The magnet coil is a superposition of six multipole coils. Each multipole coil (index q = 0,1..5) has mid plane symmetry. Only the upper half of the coil is used in the calculation. The lower half coil contributes to the vertical field B_y on the x axis (mid-plane) by a factor of 2. Each multipole coil is optimized with three 3 coil segments and their three mirror symmetric segments (for each of the n=6 poles) per pole q. Each segment m is characterized by an azimuth start angle $\Theta a_{q,m}$, a corresponding e-angle $\Theta a_{q,m}$ and a layer thickness ΔR_q. The magnetic field of an air coil in the absence of steel in a 2-D model can be calculated on the x-axis using Ampere's Law by integrating the transverse current density over each coil segment in radial and azimuthal direction:

$$B_{yn}(x) = \frac{\mu_0 \cdot \rho_n \cdot}{\pi} \cdot \sum_{q=0}^{5} I_{n,q}$$

$$I_{n,q} = \int_{\Theta a_{q,n}}^{\Theta e_{q,n}} d\theta \int_{R_n}^{R_n+\Delta R_n} r dr \frac{r(\cdot cos(\theta) - x) \cdot S_n}{r^2 + 2 \cdot r \cdot x \cdot cos(\theta) + x^2} \qquad (20)$$

$$S_n = sign(cos((n+1) \cdot \theta)$$

The parameters are:

μ_0 the free space permeability
ρ_n current density for the n-th multipole coil adjusting relative strength of the multipoles $\Delta x^{-n}/n!$
R_n, ΔR_n inner radius and thickness of multipole coil n
$\Theta a_{q,n}, \Theta e_{qn}$ the start and end azimuth angle of the three coil segments for the n^{th} multipole ($\Theta a_{0,n} = 0$)

Only the segment azimuth angles for the dipole segment $\Theta a_{qm}, \Theta e_{qm}$ have to be optimized to obtain a good dipole field. Similar quality of the multipole fields are achieved by the same segment azimuths divided by $1/n$.

Par.	n=0	n=1	n=2	n=3	n=4	n=5
ρ_n	262.1	763.6	907.2	828.7	395.2	50
R_n	70	25	12	11	10	9
ΔR_n	30	45	13	3	1	1
Θ_{n0}	0	0	0	0	0	0
Θ_{n0}	0.818	0.409	0.273	0.205	0.164	0.136
Θa_{n1}	0.863	0.431	0.288	0.216	0.173	0.144
Θe_{n1}	0.924	0.462	0.308	0.231	0.185	0.154
Θa_{n2}	1.201	0.600	0.400	0.300	0.240	0.200
Θe_{n2}	1.433	0.717	0.478	0.358	0.287	0.239

TABLE I. Parameters of the 6-layer multipole coil for exponential field (2-D optimization), ρ_n in A/mm^2, R in mm, all angles in radians

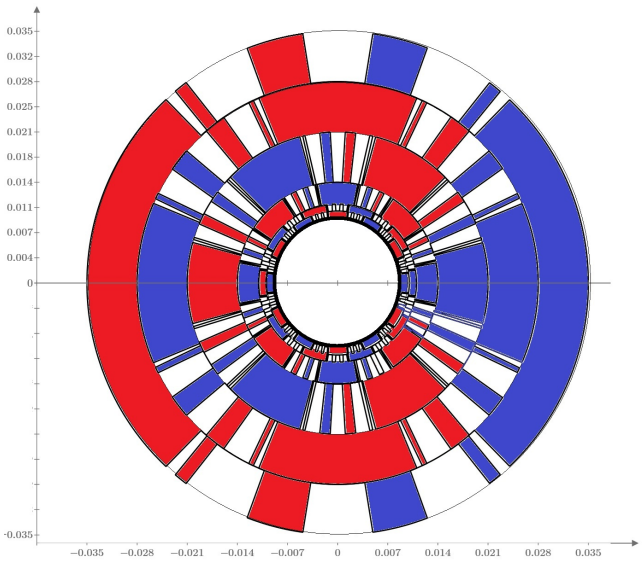

FIG. 12. Cross section of the multilayer coil of the exponential magnet

Figure 12 depicts a cross section of the magnet.

The evolution of the quadrupole field component G_y/B_y along the x-axis meets the requirement as shown in Figure 13. As shown in Table I, the current densities required for the quadrupole, sextupole, and octupole coils are close to $1000 A/mm^2$, a value that exceeds by a factor of three what can be safely achieved with superconducting magnets with Nb_3Sn wire conductor in high field even at 2K. While other material, such as the high temperature superconductor Bi_{2212} support such current densities in high fields, the mechanical stability of the superconductor, in particular the sensitivity to high mechanical stress makes its use in accelerator magnets prohibitive.

The so-called "direct wind" method for producing superconducting magnets, that have been developed at Brookhaven National Laboratory [4] is a possible technique for manufacturing the multilayer superconducting coil. This method allows -in principle- the automatized

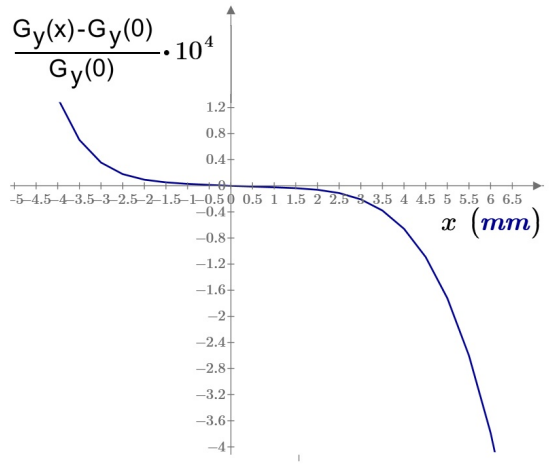

FIG. 13. The focusing gradient G_y is changing only by fraction of 10^{-3} as required

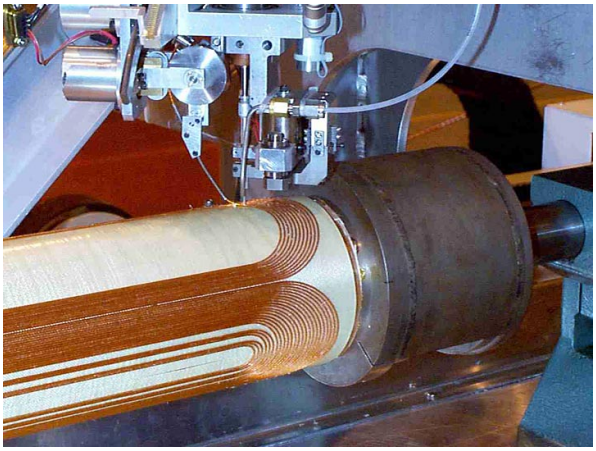

FIG. 14. Example for semi-automatic manufacturing of the coils of the superconducting final focus magnet of the HERA collider using the direct-wind method. The wire is placed with high precision by a stylus and fixed on the epoxy-coated surface by applying ultra-sonic power to the stylus (Photo courtesy of Brookhaven National Laboratory)

production of magnets with complex multilayer coils. The method would have to be developed to work with the HTC conductor envisioned for the magnets. In addition, the present method of using glass-fiber tape for collaring the superconducting coil needs to be developed for $10\,T$ magnets. Up to this point, magnets with fields up to $3.5\,T$ based on Nb-Ti superconducting wire have been built and tested successfully using this method. Figure **??** shows as an example the production of final focus magnets for the HERA collider.

In conclusion, the exponential magnet as envisioned cannot be built with presently available magnet technology and a substantial R&D program is required to develop an exponential magnet with 10 T peak field that can be mass-produced at a reasonable cost.

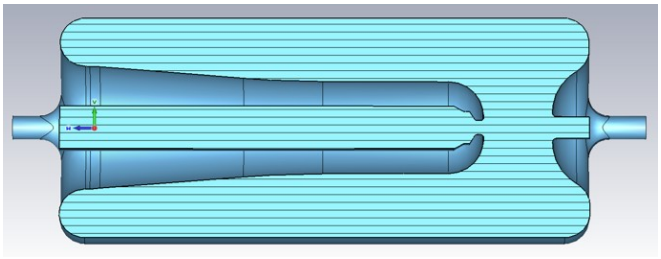

FIG. 15. Rendering of the LEReC $84\,MHz$ quarter wave length resonator. The gap length has been optimized by the resonator geometry for maximum gap voltage of $2.6\,MV$. The voltage across the gap of such cavities is limited to $2-3\,MV$ due to a maximum surface field of $E = 40\,MV/m$ at the gap. (rendering courtesy of Binping Xiao, BNL)

VIII. RF SYSTEM

The RF system required for the FFA proton driver with a total installed accelerating voltage of $> 700\,MV$ at a relatively low RF frequency of $f_{RF} = 52.13MHz$ is very demanding and the requirements for very high accelerating voltage and simultaneously fairly low RF frequency of $52.13\,MHz$ is a very uncommon constellation.

In order to fit the system in the accelerator tunnel, the low frequency cavities are envisioned to be realized by superconducting quarter-wave-resonator cavities. Such cavities have been built and one example is the passive superconducting RHIC 56-MHz bunch compression cavity. This cavity was designed for an accelerating voltage of $2\,MV$ which was achieved on the cavity test stand [6]. For optimized cavity geometry for the FFA cavity, the gap voltage is currently limited to $< 3\,MV$ on the beam axis due to the maximum surface field of $40\,MV/m$ at $2\,K$ surface temperature. A rendering of such a cavity designed for $84\,MHz$ is shown in Figure 15. The technical challenge of such cavities lies in damping of higher order modes (HOM), mechanical tuning, chemical cleaning of the cavity walls, very tight mechanical tolerances, and beam loading control. In order to provide the required voltage, a total of at least 220 such cavities each providing a voltage of $3.2\,MV$ would be needed for the desired voltage of $700\,MV$. The cavity extrapolated to a resonant frequency of $52\,MHz$ would fit into a cryostat of about $2.5\,m$ length (Note that no warm-cold transitions are required as surrounding magnets are superconducting). These cavities would fit in the available straight section space of $\simeq 840\,m$. Considerable R&D effort would be needed to design cavities with these parameters.

The present state of RF power suited for a $52\,MHz$ the art are solid state amplifiers. A 52 MHz version of this technology is commercially available. The RF installation will have to include a circulator per cavity to

accommodate some reflected power. It is expected that solid state RF power sources will continue improving in the next decade.

IX. INJECTION AND EXTRACTION

The maximum rate of high energy proton bunches extracted from the FFA would be the revolution frequency 43.48 kHz implying at every turn a new bunch is injected and a full energy bunch is extracted from the FFA. Thus 800 of the 1200 RF buckets would be occupied leaving a generous gap for kicker fall time. (Extract is from the end of the train). We still could inject more than one bunches a some terms to completely fill the ring. However, the power required to accelerate a bunch of $1 \cdot 10^{11}$ protons, our nominal design value, at a rate of $43.5\,kHz$ from 150 GeV to 500 GeV is $243\,MW$. This implies to deliver a power of $\simeq 1\,MW$ to each of the 220 $52\,MHz$ cavities which is unrealistic. Thus we have to limit the proton bunch rate to about $11\,kHz$ which implies an RF forward power coupler with a capacity of $\simeq 300\,kW$ and requires a total RF power of 62 MW.

The injection and extraction parameters discussed here are based on an acceleration time of 800 turns. Proton bunches are accelerated from $150\,GeV$ to $500\,GeV$. At any given time, 200 bunches are circulating in the FFA. The rate of extracted proton bunches is $10.9\,kHz$; which corresponds to every fourth turn a new bunch being injected and a high-energy bunch being extracted. The bunch spacing is $\Delta t_b = 115\,ns$, which corresponds to six RF wavelengths. The total beam power is $86.8\,MW$ (including the power required in the accelerator chain from $0\,GeV$ to $500\,GeV$).

Injection and extraction are accomplished using a combination of kicker and septum magnets. The kickers must provide a rectangular waveform with rise and fall times shorter than $100\,ns$. Four kicker magnets, each located in a straight section of approximately $3\,m$ length and providing a kick of $1\,mrad$, generate the required total deflection. The beam is first kicked outward into a region with a stronger focusing field, which deflects the beam toward the lower-field region. Once in the lower-field region, subsequent kicks further deflect the beam toward the low-field aperture.

The extraction orbit evolves differently from an orbit in a linear magnetic field. Once the beam has entered the lower-field region on the inside, it is not deflected back into the high-field aperture. This is a characteristic feature of exponential-field magnets and facilitates beam extraction.

Each straight-section magnet along the path of the extracted beam, with a length of $80\,cm$, must provide an enlarged aperture on the low-field side to accommodate the exiting

beam. After the fourth kicker magnet, the beam is sufficiently deflected to pass through the insulating vacuum between the coil and collar of a focusing magnet. Downstream of this magnet, a $3\,m$ septum provides an additional deflection of $9\,mrad$, allowing the beam to be steered away from the FFA.

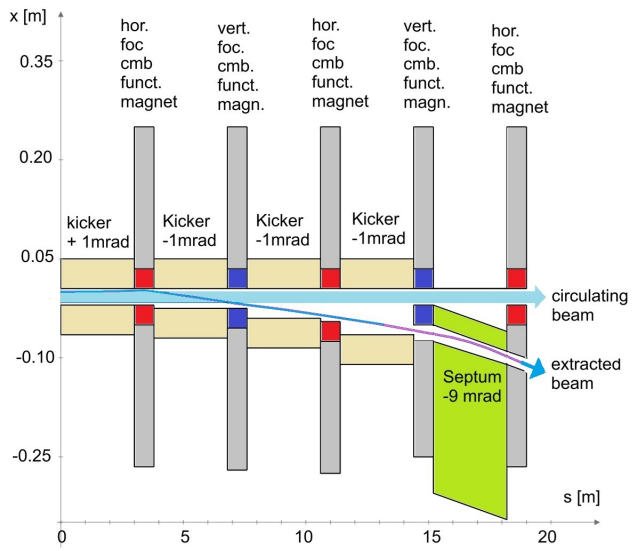

FIG. 16. Schematic layout of the extraction system. Four $1\,mrad$ kicker magnets placed between the combined-function magnets— the first providing a positive kick and the others radially inward kicks—transport the $500\,GeV$ beam to $x = -60\,mm$, which is sufficient for extraction. The extracted beam passes through the insulating vacuum of the downstream superconducting magnet. The circulating beam trajectory is shown as a straight reference line, and all elements in the figure are drawn relative to this straight trajectory.

The extracted beam interferes with the cryostat envelope of subsequent superconducting magnets. This presents a significant technical challenge, as the beam must pass through the insulating vacuum region of several downstream magnets. The design of these magnets must therefore accommodate the extracted beam trajectory.

To ensure technical feasibility, the kicker magnets must be segmented. The kickers are assumed to employ ferrite yokes with a vertical gap height of $h_{gap} = 15\,mm$. The horizontal kicker aperture w_{gap} varies between $20\,mm$ and $65\,mm$. Kickers one and two each consist of ten segments of $0.3\,m$ length, whereas kicker three consists of 15 segments and kicker four of 20 segments.

The voltage required to drive the excitation current of $8\,kA$, corresponding to a field rise time of $100\,ns$, varies between $V_{kicker} = 40\,kV$ and $V_{kicker} = 65\,kV$. This estimate includes approximately 20% eddy-current losses in the conductor. Although technically demanding, such pulsed magnet systems are within present technological capabilities. A preliminary layout of the extraction system is shown in Fig. 16.

X. NEXT STEP STUDY PLAN

This study provides only a first assessment of a possible application of a fixed field accelerator (FFA) for generating a continuous stream of high-energy proton bunches that could be used to drive plasma wakefield acceleration of electrons for an e^+e^- collider. The parameters developed in this work are internally consistent but far from optimal. To make further progress toward establishing feasibility, a comprehensive numerical optimization effort is required.

Moreover, it is expected that, even after substantial optimization, the required performance of magnets, RF systems, and pulsed power devices may exceed the capabilities of present-day accelerator technology. Consequently, a comprehensive technical R&D program will be required before such a facility could be realized.

A large number of studies, conceptual design efforts, and R&D activities must therefore be undertaken before this scheme can be considered technically feasible. The main study topics include:

- Optimization of design parameters to support technical feasibility
- Development of complete linear beam optics, including transitions between arcs and straight sections
- Optimization of the accelerator trajectory to fit the FFA into an existing accelerator tunnel
- Comprehensive studies of nonlinear beam dynamics
- Start-to-end six-dimensional symplectic accelerator modeling of the acceleration process
- Assessment of collective effects during acceleration and during and after bunch compression
- Evaluation of the impact of magnetic field and alignment errors and the development of corresponding correction schemes
- Orbit control and stabilization

Conceptual hardware design studies include:

- Conceptual design of superconducting magnets
- Studies of suitable superconducting wire technologies
- Conceptual design of superconducting RF cavities
- RF power system design studies
- Conceptual design of pulsed magnets

Another important consideration is cost. The FFA configuration envisioned here is likely to be very expensive, and its cost must be evaluated and compared with alternative approaches. The corresponding studies should include:

- Conceptual cost estimate for an optimized FFA-based solution
- Investigation of alternative accelerator concepts with comparable performance, such as stacked rapid-cycling synchrotrons or recirculating linacs
- Comparative cost analysis of the FFA approach and alternative solutions

XI. CONCLUSION

This study demonstrates that a proton driver based on fixed field accelerator (FFA) technology is, in principle, feasible. The FFA configuration developed as part of this study represents one possible solution. However, there remains considerable scope for further optimization, which may lead to an improved FFA design suitable as a basis for a detailed assessment of technical feasibility. The evaluation presented here is at a preliminary stage, and a comprehensive study program will be required to progress toward a conceptual design and to define a focused R&D program.

The primary objective of the ALIVE Study [2] is to explore a pathway toward an affordable next-generation collider facility for High Energy Physics. The analysis presented in this report indicates that the cost of an FFA-based proton driver may be substantial, primarily due to the unconventional lattice configuration and the large number of required RF cavities and associated RF power systems. It is therefore important to further evaluate the cost implications of the FFA-based approach and to compare it with alternative proton driver concepts that could provide similar performance.

The FFA scheme studied in this report may also have applications beyond proton-driven plasma wakefield acceleration.

Neutron spallation sources represent one potential application, as they rely on a continuous high-intensity proton beam that could potentially be generated efficiently with an FFA.

Fixed target experiments might also benefit from the higher event rates achievable by replacing the driver synchrotron with an FFA.

In conclusion, the results of this study suggest that high-energy proton acceleration using fixed field accelerators is a promising concept, and further investigations are well justified.

Acknowledgments

The author acknowledges benefiting from discussions with Stephen Brooks, Scott Berg, Binping Xiao, Wencan Xu, and Alex Saltsman, Qiong Wu, Ramesh Gupta (BNL), and Georg Hoffstaetter de Torquat (Cornell University). Michael Koratzinos from CERN made interesting remarks concerning the exponential magnet design. I am obliged to Allen Caldwell and Matthew Wing for

carefully reading the manuscript and providing helpful comments.

REFERENCES

[1] AWAKE Collaboration. "Acceleration of electrons in the plasma wakefield of a proton bunch". In: *Nature* 561.7723 (2018), pp. 363–367. ISSN: 1476-4687. DOI: 10.1038/s41586-018-0485-4. URL: https://doi.org/10.1038/s41586-018-0485-4.

[2] Allen Caldwell et al. *Proton-Driven Plasma Wakefield Acceleration for Future HEP Colliders*. 2025. arXiv: 2503.21669 [physics.acc-ph]. URL: https://arxiv.org/abs/2503.21669.

[3] Carl A Lindstroem. "Staging of Plasma Wakefield Acceleration". In: *Physysicl Review of Accelerators and Beams* DIS2019 (2021), p. 20. DOI: DOI:10.1103/PhysRevAccelBeams.24.014801.

[4] Brett Parker et al. "BNL Direct Wind Superconducting Magnets". In: *IEEE Trans. Appl. Supercond.* 22.3 (2012). Ed. by Neil Mitchell, p. 4101604. DOI: 10.1109/TASC.2011.2175693.

[5] K. R. Symon et al. "Fixed-Field Alternating-Gradient Particle Accelerators". In: *Phys. Rev.* 103 (6 Sept. 1956), pp. 1837–1859. DOI: 10.1103/PhysRev.103.1837. URL: https://link.aps.org/doi/10.1103/PhysRev.103.1837.

[6] Q. Wu et al. "Operation of the 56 MHz Superconducting RF Cavity in RHIC with Higher Order Mode Damper". In: *Phys. Rev. Accel. Beams* 22.10 (2019), p. 102001. DOI: 10.1103/PhysRevAccelBeams.22.102001. arXiv: 1805.01531 [physics.acc-ph].